THE JOURNAL OF BIOLOGICAL CHEMISTRY VOL. 291, NO. 47, pp. 24390–24405, November 18, 2016


# Microvesicle-mediated Wnt/β-Catenin Signaling Promotes Interspecies Mammary Stem/Progenitor Cell Growth*

Received for publication, March 7, 2016, and in revised form, October 2, 2016 Published, JBC Papers in Press, October 12, 2016, DOI 10.1074/jbc.M116.726117

Leen Bussche[‡1,2], Gat Rauner[‡1], Marc Antonyak[§], Bethany Syracuse[‡], Melissa McDowell[‡], Anthony M. C. Brown[¶], Richard A. Cerione[§], and Gerlinde R. Van de Walle[‡3]

*From the [‡]Baker Institute for Animal Health and [§]Department of Molecular Medicine, College of Veterinary Medicine, Cornell University, Ithaca, New York 14853 and the [¶]Department of Cell & Developmental Biology, Weill Cornell Medical College, New York, New York 10065*

**Edited by Thomas Söllner**

**Signaling mechanisms that regulate mammary stem/progenitor cell (MaSC) self-renewal are essential for developmental changes that occur in the mammary gland during pregnancy, lactation, and involution. We observed that equine MaSCs (eMaSCs) maintain their growth potential in culture for an indefinite period, whereas canine MaSCs (cMaSCs) lose their growth potential in long term cultures. We then used this system to investigate the role of microvesicles (MVs) in promoting self-renewal properties. We found that Wnt3a and Wnt1 were expressed at higher levels in MVs isolated from eMaSCs compared with those from cMaSCs. Furthermore, eMaSC-MVs were able to induce Wnt/β-catenin signaling in different target cells, including cMaSCs. Interestingly, the induction of Wnt/β-catenin signaling in cMaSCs was prolonged when using eMaSC-MVs compared with recombinant Wnt proteins, indicating that MVs are not only important for transport of Wnt proteins, but they also enhance their signaling activity. Finally, we demonstrate that the eMaSC-MVs-mediated activation of the Wnt/β-catenin signaling pathway in cMaSCs significantly improves the ability of cMaSCs to grow as mammospheres and, importantly, that this effect is abolished when eMaSC-MVs are treated with Wnt ligand inhibitors. This suggests that this novel form of intercellular communication plays an important role in self-renewal.**

The mammary gland in humans and other mammals is a dynamic organ that undergoes significant developmental changes during pregnancy, lactation, and involution. It is generally accepted that the cellular repertoire of the human mammary gland is generated by stem cells (1). These cells, commonly referred to as mammary stem/progenitor cells (MaSCs),[4] have a unique capacity for self-renewal, as well as for generating the three lineages that comprise the lobulo-alveolar structure of the adult gland (1). Determining the nature of the signals that regulate growth and self-renewal of MaSCs is of central importance for understanding developmental changes in the mammary gland and possibly for targeting stem-like cells in breast cancer (2). Studying these signals has been complicated because mammosphere cultures derived from mammary tissue samples lose their ability to self-renew over time, at least in humans (3).

Several signaling pathways have been implicated in the regulation of stem cell self-renewal, including those triggered by Wnt/β-catenin, Notch, Hedgehog, TGF-β, EGF receptor, phosphatase and tensin homolog, and polycomb complex protein (Bmi-1) (4–12). Of these pathways, the Wnt signaling pathway plays a critical role in regulating murine growth (13). Wnt proteins comprise a major family of signaling molecules involved in a myriad of cell biological and developmental processes. Distinct Wnt signaling pathways have been identified, including the canonical or Wnt/β-catenin-dependent pathway and non-canonical, β-catenin-independent, pathways. The latter have been further divided into planar cell polarity, Wnt/$Ca^{2+}$ pathways, and others (14, 15). Wnt1 and Wnt3a are examples of ligands that activate the canonical Wnt/β-catenin signaling pathway, whereas Wnt5a typically signals via the non-canonical, β-catenin-independent pathway. Both canonical and non-canonical Wnt signals have been shown to promote stem cell activity in mammosphere assays (16). However, key questions remain with regard to the mechanisms that regulate this outcome. Because Wnt proteins are highly hydrophobic because of lipid modifications, they face critical obstacles in traveling in the extracellular space for long range signaling (17). Packaging purified Wnt proteins into lipid vesicles has been shown to enhance and sustain Wnt signaling *in vitro* and to result into robust biological activity *in vivo* (18). Extracellular vesicles (EVs) represent another type of vesicle that improves Wnt dispersal in the extracellular matrix, based on their stable nature and ability to travel over long distances. This makes EVs an ideal platform for integrating and transmitting signaling

* This work was supported by National Institutes of Health Grant R21 CA186981 (to A. M. C. B.). The authors declare that they have no conflicts of interest with the contents of this article. The content is solely the responsibility of the authors and does not necessarily represent the official views of the National Institutes of Health.

[1] Both authors contributed equally to this work.

[2] Postdoctoral fellow of the Belgian American Education Foundation.

[3] To whom correspondence should be addressed: Hungerford Hill Rd., Ithaca, NY 14853. Tel.: 607-256-5649; Fax: 607-256-5608; E-mail: grv23@cornell.edu.

[4] The abbreviations used are: MaSC, mammary stem/progenitor cell; eMaSC, equine MaSC; cMaSC, canine MaSC; MV, microvesicles; EV, extracellular vesicles; CM, conditioned medium; PDT, population doubling time; GSK3β, glycogen synthase kinase 3β; p-Dvl-2, phosphorylated Dishevelled-2; PM-GFP, plasma membrane-targeted GFP; ABC, active β-catenin; r, recombinant; TCF/LEF, T-cell factor/lymphoid enhancer factor; EpSC, epithelial stem cell.

molecules and other cytosolic proteins, as well as lipids and RNA, between cells (19). Thus far, EVs derived from fibroblast L-Wnt3a cells, human colon cancer Caco-2 cells, and lymphoma SP cells have been shown to act as couriers carrying Wnt ligands (17, 20, 21). EVs are composed of exosomes and microvesicles (MVs), which differ in size and mechanism of formation. Exosomes are derived from multivesicular bodies and range in size from 30 to 100 nm, whereas MVs are considerably larger (0.2–2 $\mu$m in diameter) and are shed from the plasma membrane via budding (19). Both exosomes and MVs have the ability to transfer their content to other cells, often leading to signaling events in the recipient cells that influence their behavior. The role of EVs in transferring Wnt signals between MaSCs, however, has not previously been explored.

Our laboratory has focused on studying the self-renewal capacities of MaSCs isolated from a variety of mammalian species (22), and this comparative approach allows us to initiate studies on self-renewal signaling in and between MaSCs. In these studies, we made the recurrent observation that MaSCs of canine origin (cMaSCs) lose their expansion capacity in long term cultures, whereas MaSCs of equine origin (eMaSCs) do not, and this led us to formulate the hypothesis that a difference in self-renewal-associated cargo in MVs might explain this striking difference in long term expansion capacity. Our salient findings were that Wnt1 and especially Wnt3a were expressed at higher levels in MVs from eMaSCs compared with MVs from cMaSCs. Furthermore, we were able to show that eMaSC-MV induced a sustained activation of the Wnt/$\beta$-catenin signaling pathway in target cells, including cMaSCs. In addition, the MV-mediated activation of the Wnt/$\beta$-catenin signaling pathway significantly improved the ability of cMaSCs to grow as mammospheres. Taken together, these data provide strong evidence that MVs provide a novel mechanism through which MaSCs communicate to promote self-renewal.

## Results

*MaSCs Derived from Canine and Equine Origin Show Striking Differences in Expansion Capacities*—When cultivating canine and equine MaSCs, we consistently found that cMaSCs lose their expansion capacity in long term adherent cell cultures, whereas eMaSCs maintain their expansion capacity for an indefinite period, as determined by population doubling time (PDT) analyses (Fig. 1*A*). To investigate this difference in growth kinetics, serial mammosphere assays were performed to evaluate the self-renewal capacity of these mammary cell cultures (16, 23). We found that eMaSCs were consistently able to form mammospheres after serial passaging in ultra low attachment plates, whereas cMaSCs were unable to form mammospheres beyond passage 8 (Fig. 1*B*). We next examined whether factors released by eMaSCs into the medium could account for their sustained growth by cultivating cMaSCs in the presence of conditioned medium from eMaSCs (eMaSC-CM). This resulted in a remarkable improvement of the growth capacity of cMaSCs over time (Fig. 1*C*, *left panel*), indicating that eMaSCs produce factors that can stimulate MaSC growth. In contrast, control experiments in which cMaSCs were cultivated in their own CM did not improve their growth capacity over time (Fig. 1*C*, *left panel*). Moreover, culturing eMaSCs either in the presence of their own CM or in the presence of cMaSC-CM did not change their expansion capacity in long term adherent cell cultures when compared with control cell culture medium (Fig. 1*C*, *right panel*).

*MaSCs Produce MVs*—In view of evidence that MVs, a subclass of EVs ranging in size between 0.2 and 2 $\mu$m in diameter, can function as an important cell to cell communication mechanism, we explored whether MVs could play a role in the growth expansion of MaSCs. To the best of our knowledge, only one recent study has described the secretion of EVs by human MaSCs. In that instance cells were grown in short term mammosphere cultures, and only EVs smaller than 220 nm were analyzed (24). Because most MVs are larger than 220 nm, we first isolated and characterized the MVs secreted by eMaSCs and/or cMaSCs. The procedure for isolating MVs from MaSCs is schematically shown in Fig. 2*A*. First, following removal of cells and debris by differential centrifugation, the CM of MaSCs was analyzed by dynamic light scattering, and two distinct peaks, averaging ~15 and ~250 nm, were observed for both species (Fig. 2*B*, *panel i*). In addition, the fluorescent dye FM1–43FX was used to label plasma membranes, and particles of different sizes decorating the cell surface of eMaSCs and cMaSCs were observed (Fig. 2*B*, *panel ii*). Next, the partially clarified CM was filtered using a 0.22-$\mu$m filter, and a pure and homogeneous preparation of MVs was recovered from MaSCs and visualized using FM1–43FX staining (Fig. 2*C*, *panel i*) and with a size of ~400 nM as analyzed by dynamic light scattering (Fig. 2*C*, *panel ii*). Further characterization of the isolated MVs, using a combination of flow cytometry and Western blotting, showed that they were positive for the vesicle markers flotillin-2 and CD81 but lacked RhoA. The latter serves as a negative control because it is not a specific MV cargo protein (Fig. 2*D*, *panels i* and *ii*).

*eMaSC-MV Can Transfer Their Cargo to cMaSCs*—Given that culturing cMaSCs with eMaSC-CM caused a remarkable increase in growth capacity over time (Fig. 1*C*) and MVs were shown to be present in eMaSC-CM, we next asked whether the MVs in the CM were responsible for this effect. First, to determine whether the cargo in eMaSC-MVs could be transferred to cMaSCs, we transfected eMaSCs with a plasmid encoding a plasma membrane-targeted GFP (PM-GFP) (Fig. 3*A*, *panel i*). MVs collected from PM-GFP-transfected eMaSCs showed clear incorporation of PM-GFP, as indicated by Western blotting analyses (Fig. 3*A*, *panel ii*). Importantly, addition of eMaSC-derived PM-GFP-expressing MVs to cMaSC cultures induced GFP fluorescence in the cMaSCs, indicating that MVs from eMaSCs are indeed capable of transferring their cargo to recipient cells (Fig. 3*A*, *panel iii*). The percentage of GFP-positive cMaSCs was 26.2 $\pm$ 19.0%. Next, we repeated our original cultivation experiments in which cMaSCs were cultured in the presence of eMaSC-CM, but purified eMaSC-MVs were used instead of CM. We found that cMaSCs cultured with eMaSC-MVs showed a remarkable improvement in their growth capacity over time, similar to that observed with eMaSC-CM (Fig. 3*B*). Taken together, these observations indicate that eMaSC-MVs are capable of transferring their cargo to recipient cMaSCs and promote MaSC growth.

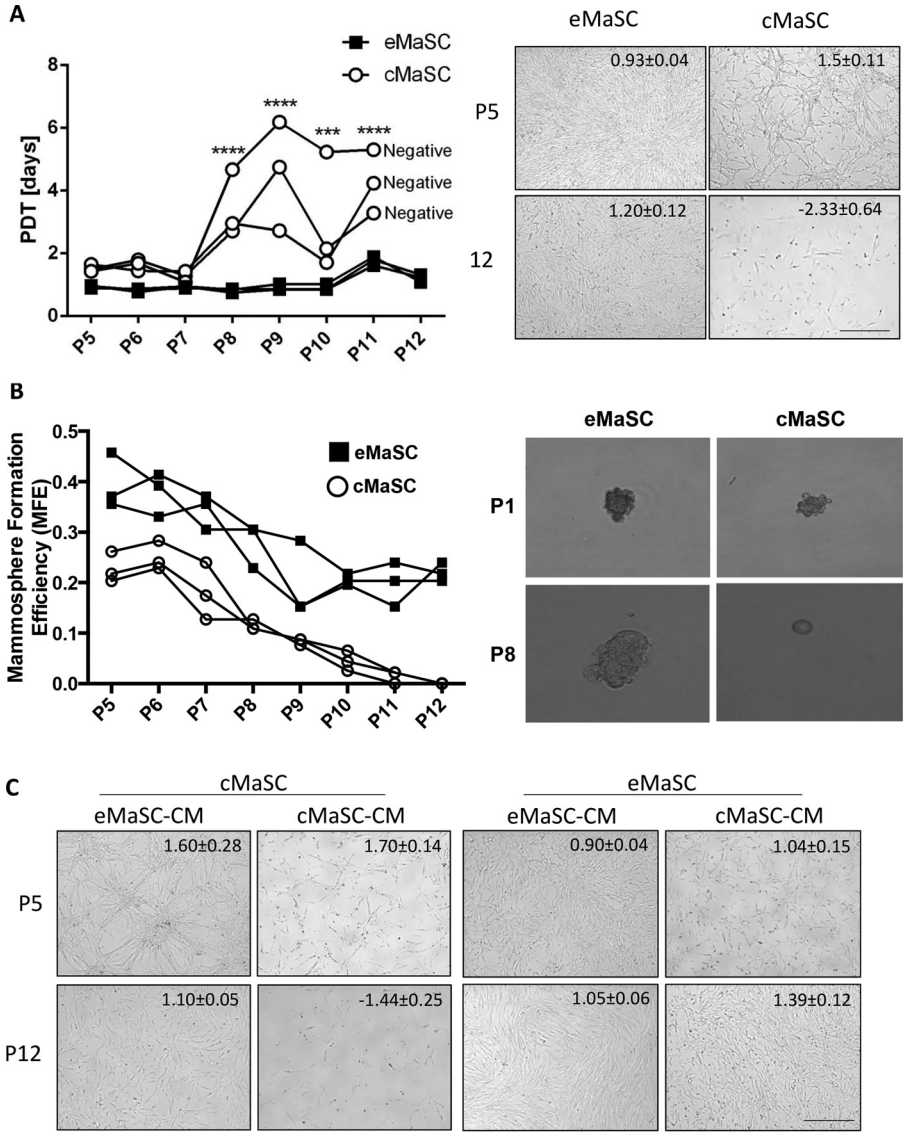


FIGURE 1. **eMaSC-derived CM rescues the growth potential of cMaSCs.** *A*, *left panel*, PDT were calculated from adherent cell cultures of eMaSCs (*squares*) and cMaSCs (*circles*) between P5 and P11 ($n = 3$). ***, $p < 0.001$; ****, $p < 0.0001$. *Negative* indicates that cells stopped dividing. *Right panel*, representative images of adherent eMaSCs and cMaSCs at P5 (*upper row*) and P12 (*lower row*) are shown with matching PDT ± STDEV for each image. *Scale bar*, 50 μm. *B*, secondary mammospheres were counted 1 week after plating dissociated eMaSCs and cMaSCs, originally obtained from adherent cultures between P5 and P12, on ultra low attachment plates ($n = 3$). Representative images of mammosphere formation of P1 and P8 eMaSCs and cMaSCs are shown. *C*, cMaSCs and eMaSCs were cultured either in their own CM or in CM from the other species ($n = 3$). Images at P5 (low) and P12 (high) maintained under each condition are shown with matching PDT ± STDEV for each image. *Scale bar*, 50 μm.

*Wnt-related Cargo Is Differentially Expressed in MVs Generated by eMaSCs and cMaSCs*—To identify factors present in the eMaSC-MVs that are responsible for promoting the growth and self-renewal of cMaSCs, we compared the proteome profiles of MVs isolated from eMaSCs and cMaSCs using LC-MS/MS analysis. As expected, a major group of proteins present in the MaSC-MVs were cytoskeletal proteins such as actin, tubulin, vimentin, and heat shock proteins (Fig. 4*A*). More interestingly, several proteins associated with key pathways related to stem cell maintenance and differentiation, such as EGF receptor, FGF, and Wnt signaling pathways, were differentially expressed in MVs from eMaSCs *versus* cMaSCs (Fig. 4*B*). Because Wnt signaling has been implicated in promoting stem cell growth in mammospheres (16), we hypothesized that a difference in MV-mediated Wnt signaling between eMaSCs and cMaSCs might explain the observed difference in mammosphere growth between these two cell populations (Fig. 1*B*). To validate the differential expression of proteins associated with the Wnt signaling pathway in the MVs of eMaSCs and cMaSCs, we first examined directly the protein levels of Wnt1, Wnt3a, Wnt5a, and the Wnt antagonist Dkk1 in the MVs. We found that Wnt1 and Wnt3a, ligands that activate the Wnt/β-catenin signaling pathway, were expressed at higher levels in MVs of eMaSCs, compared with cMaSCs (Fig. 4*C*). In contrast, Wnt5a, which typically signals via non-canonical, β-catenin-independent pathways (16), was equally expressed in MVs collected from both species (Fig. 4*C*). In addition, Dkk1, a specific negative regulator of Wnt/β-catenin signaling, was present in MVs from cMaSCs but not eMaSCs (Fig. 4*C*). These findings suggested a clear difference in the Wnt signaling-related

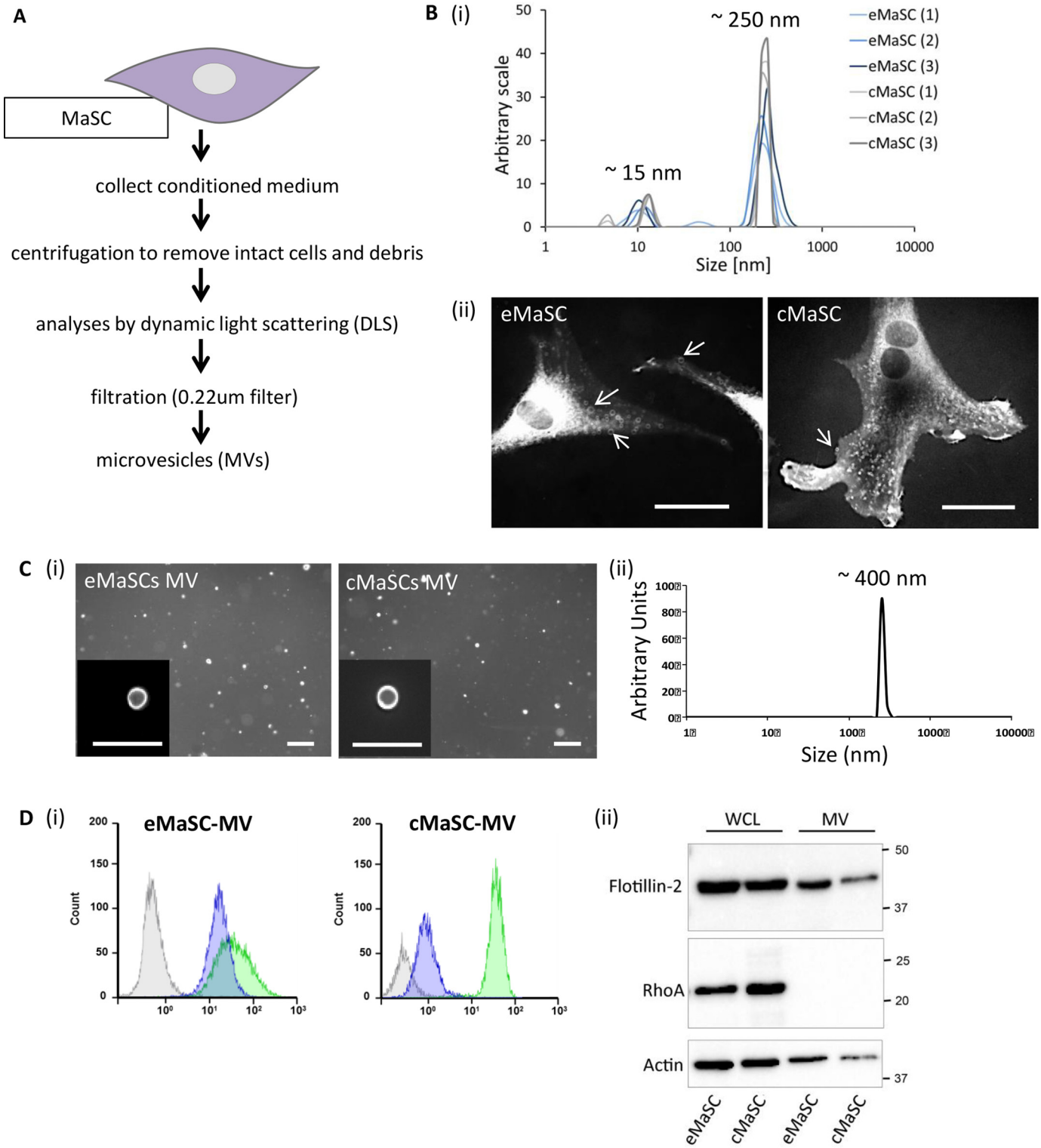


FIGURE 2. **eMaSCs and cMaSCs generate MVs.** *A*, schematic overview of procedure for isolating MVs from CM. *B*, *panel i*, dynamic light scattering plots of MaSC-CM clarified of cells and debris, with ~15- and ~250-nm peaks. A histogram of six independent experiments (three eMaSC-CM and three cMaSC-CM isolations) is shown. *Panel ii*, fluorescent microscopy of eMaSCs and cMaSCs stained with the membrane dye FM1–43FX. Vesicles of different sizes decorating the MaSC surface are visible. *Scale bars*, 10 $\mu$m. *C*, *panel i*, fluorescent microscopy of MVs isolated from eMaSCs and cMaSCs stained with FM1–43FX. *Insets*, high magnification of individual MVs. *Scale bars*, 1 $\mu$m. *Panel ii*, dynamic light scattering plot of MaSC-MVs isolated from MaSC-CM via filtration, with a ~400-nm peak. *D*, *panel i*, the presence of CD81 (*green*) and flotillin-2 (*purple*) on MaSC-MVs was determined by flow cytometry. *Gray* represents isotype controls. A representative histogram of three independent experiments is shown. *Panel ii*, MVs isolated from MaSCs were immunoblotted for the MV-marker flotillin-2 (*top panel*), the cytosolic-specific marker RhoA (*middle panel*), and loading control $\beta$-actin (*bottom panel*). A representative Western blot image is shown of three independent experiments ($n = 3$).

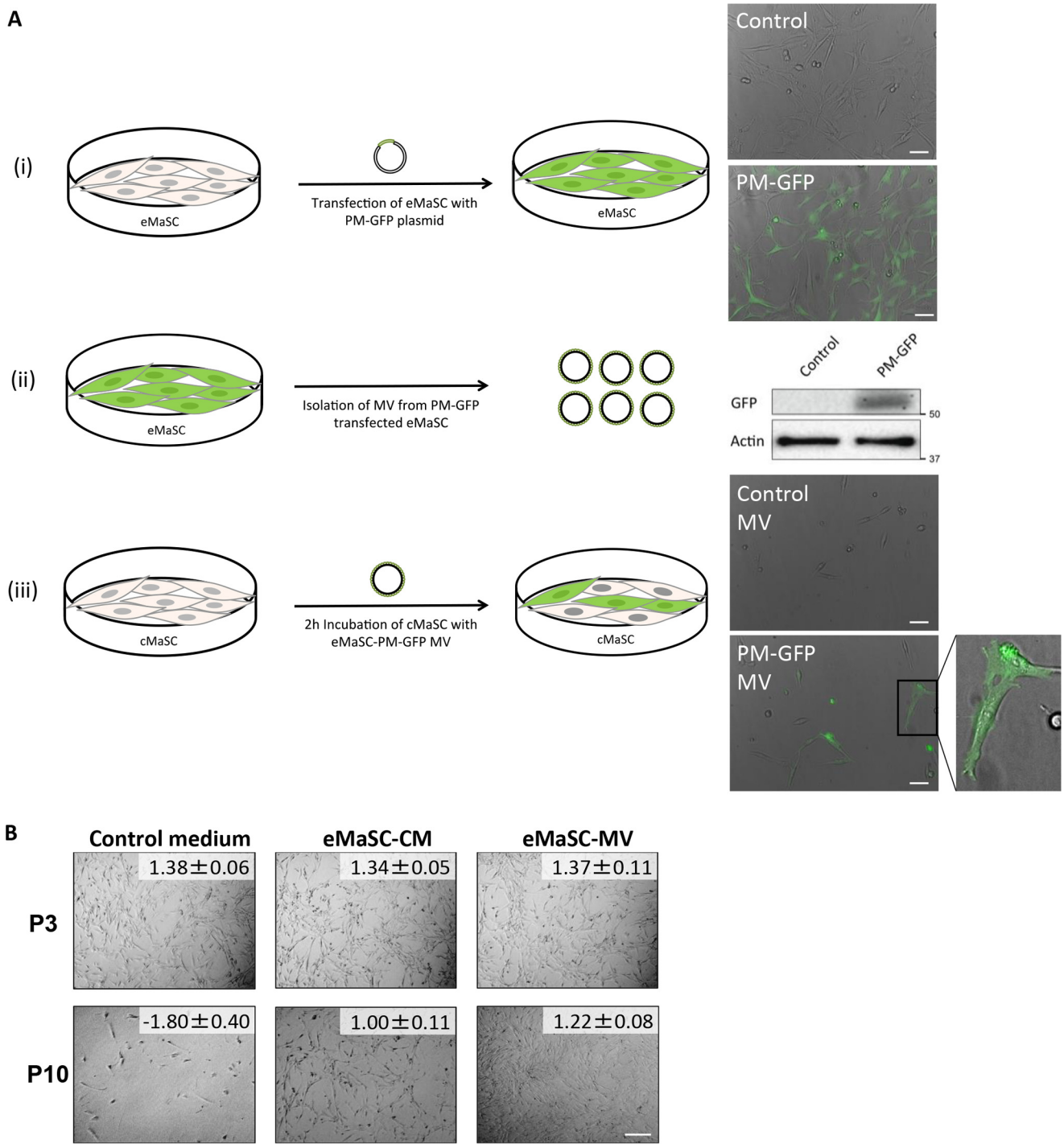


FIGURE 3. **eMaSC-MVs transfer their cargo to cMaSCs and restore cMaSC growth in adherent cultures.** *A*, description and results of experiments conducted to demonstrate that MVs can transfer cargo from eMaSCs to cMaSCs. *Panel i*, fluorescent microscopy of mock (control) and PM-GFP (PM-GFP) transfected eMaSCs. *Scale bars*, 50 $\mu$m. *Panel ii*, immunoblots for GFP show that PM-GFP was incorporated into MVs generated from PM-GFP transfected eMaSCs. $\beta$-actin was included as loading control. A representative Western blot image is shown of three independent experiments ($n = 3$). *Panel iii*, fluorescent microscopy shows that incubation of cMaSCs with MVs generated from PM-GFP transfected eMaSCs for 2 h results in GFP-positive cells. *Inset*, high magnification of individual GFP-positive cMaSCs. *Scale bars*, 50 $\mu$m. *B*, representative images of P3 and P10 cMaSCs cultured in control medium, eMaSC-CM or eMaSC-MVs, with matching PDT ± STDEV for each image. *Scale bar*, 100 $\mu$m.

proteins contained in MVs derived from eMaSCs and cMaSCs.

*eMaSCs Have Inherently More Active Wnt/β-Catenin Signaling Potential than cMaSCs*—Before elucidating the role of Wnt proteins in MVs in more detail, we first wished to confirm that the Wnt/β-catenin signaling pathway is actually present in the recipient MaSCs. To this end, both eMaSCs and cMaSCs were cultured over multiple passages, and the levels of active β-catenin (ABC), a hallmark of the Wnt/β-catenin signaling pathway (25–27), and phosphorylated Dishevelled-2 (p-Dvl-2), which is induced by Wnt1, Wnt3s, and Wnt5a, were determined by Western blotting analyses. ABC could be detected in

**A** **10 most abundant proteins in MaSC-MV**

| | eMaSC-MV | cMaSC-MV |
|---|---|---|
| 1 | Collagen type I | Vimentin |
| 2 | Beta-actin | Filamin A |
| 3 | Fibronectin | Collagen alpha-2 chain precursor |
| 4 | Collagen type VI | Beta-actin |
| 5 | Sperm-membrane associated protein P47 | Myosin 9 |
| 6 | Cytokeratin 9 | Alpha-actin |
| 7 | Keratin 1 | Cytokeratin 9 |
| 8 | Vimentin | Keratin 1 |
| 9 | Tenascin | Annexin A2 |
| 10 | Glyceraldehyde-3-phosphate dehydrogenase | Collagen alpha-1 chain precursor |

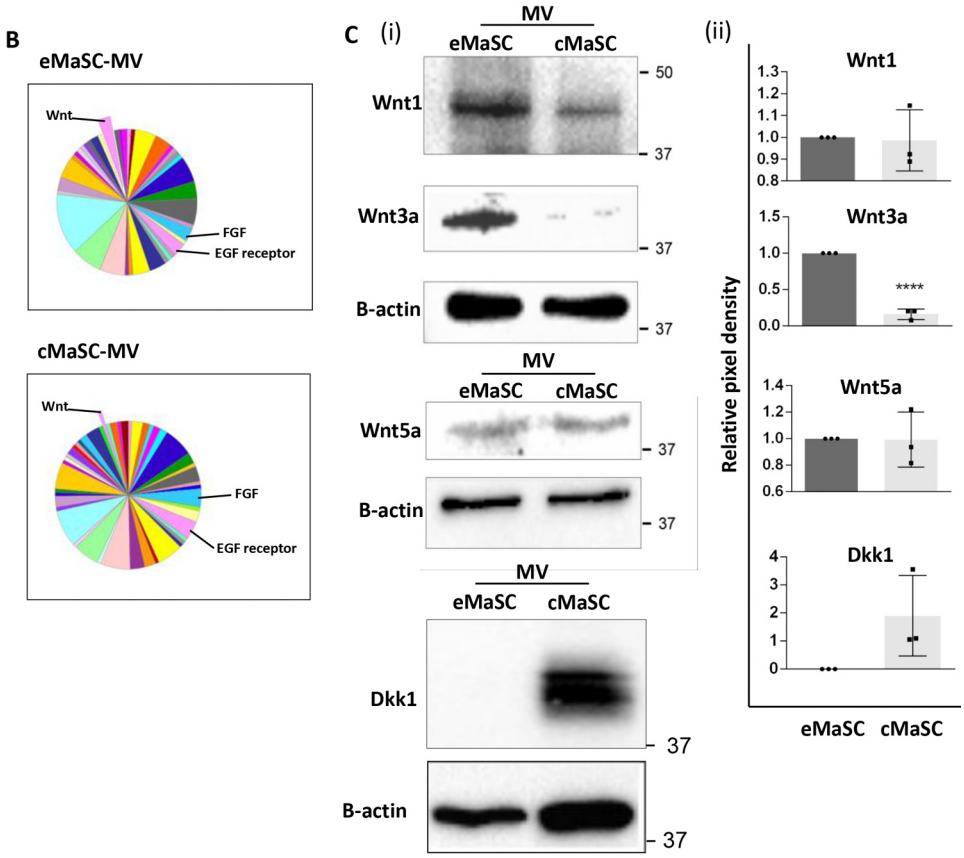


FIGURE 4. **Wnt-related cargo differs between eMaSC-MVs and cMaSC-MVs.** *A*, mass spectrometry was performed on MVs isolated from eMaSCs and cMaSCs. The 10 most abundant proteins identified are listed. *B*, PANTHER-generated pathway pie charts of LC/MS/MS-identified proteins in eMaSC-MVs and cMaSC-MVs. Proteins involved in FGF, EGF receptor, and Wnt signaling were detected in MVs of both cell types. *C*, MV lysates were immunoblotted as indicated. Note that Wnt1 and Wnt3a were more abundant in MVs from eMaSCs compared with cMaSCs, whereas Dkk1 was present in MVs from cMaSCs but not eMaSCs. Western blot images of three independent experiments were quantified using the Bio-Rad ChemiDoc MP system (*panel ii*), and a representative Western blot image is shown (*panel i*; $n = 3$). ****, $p < 0.0001$.

both low and high passage eMaSC cultures, whereas ABC was only detected in low passages of cMaSCs (Fig. 5*A*, *panel i*, *top panel*). A similar observation was made for p-Dvl-2, with phosphorylated Dvl-2 detected in all passages of eMaSCs, but only in low passage cMaSCs (Fig. 5*A*, *panel i*, *middle panel*). To corroborate these findings, we analyzed active Wnt/β-catenin signaling in high passage eMaSC and cMaSC cultures by studying the nuclear localization of β-catenin (Fig. 5*B*). In response to Wnt/β-catenin signaling, cytoplasmic β-catenin translocates to the nucleus to act as a transcriptional coactivator (28). The percentage of cells expressing nuclear β-catenin in high passage eMaSCs was similar to that of Rat2/Wnt1 cells, which stably express exogenous Wnt1 and have constitutive activation of Wnt signaling (29) (95.7 ± 7.6 and 94.8 ± 9.0, means ± S.D., respectively). In contrast, nuclear β-catenin localization in high passage cMaSCs was significantly lower compared with high passage eMaSCs and comparable with that of control Rat2/MV7 cells, which do not have activated Wnt signaling (6.5 ± 11.7 and 14.5 ± 6.0, means ± S.D., respectively). Sequestration of glycogen synthase kinase 3β (GSK3β), a member of the β-catenin destruction complex (30), from the cytosol into multivesicular bodies, has been shown to regulate Wnt activity (31). To evaluate GSK3β expression in high passage eMaSCs and cMaSCs, immunofluorescence was performed on cells at days 1

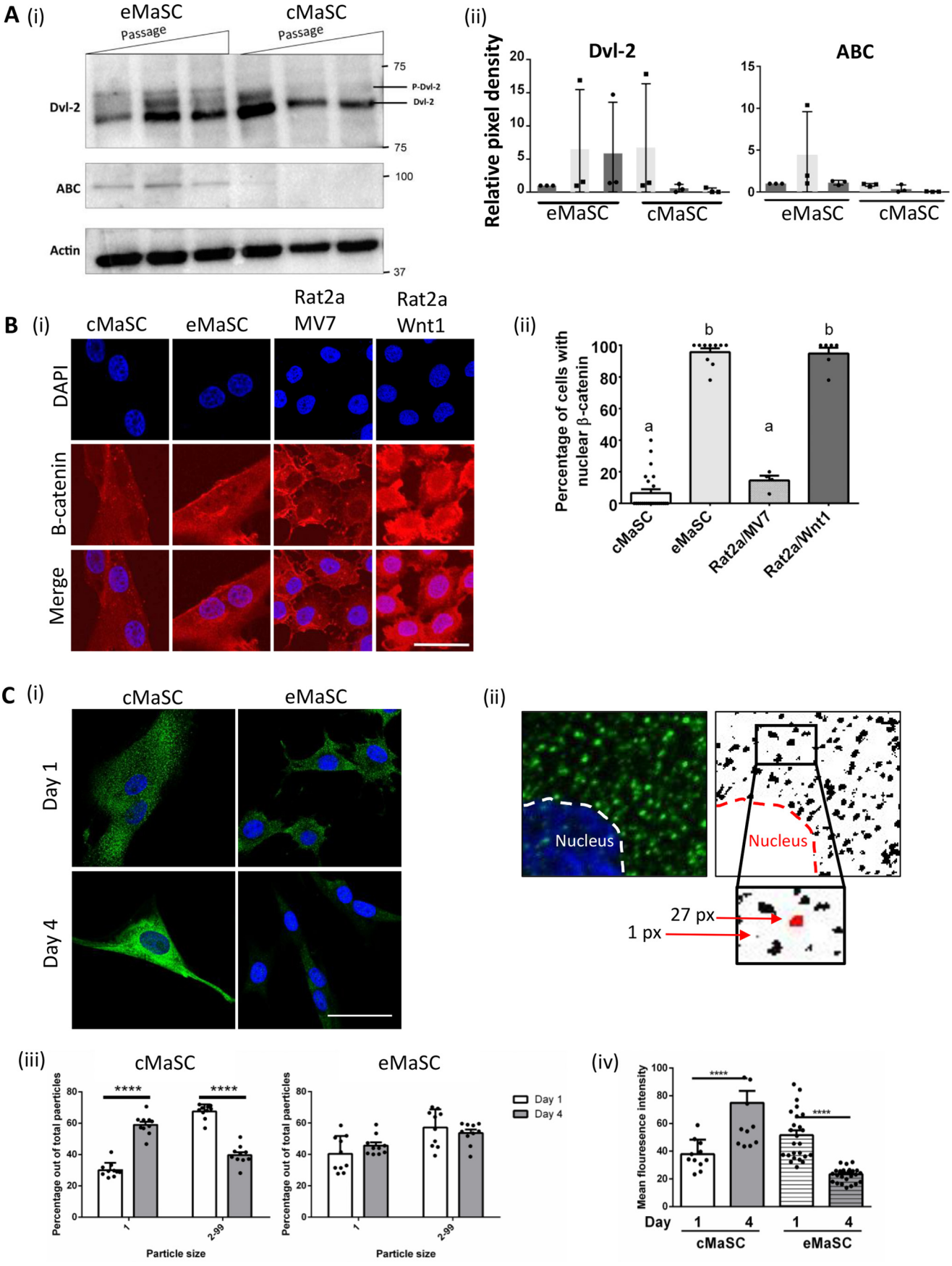
A (i)
eMaSC
cMaSC
Passage
Passage
Dvl-2
ABC
Actin
75
P-Dvl-2
Dvl-2
75
100
37
(ii)
Relative pixel density
Dvl-2
ABC
eMaSC
cMaSC
eMaSC
cMaSC
B (i)
cMaSC
eMaSC
Rat2a MV7
Rat2a Wnt1
DAPI
B-catenin
Merge
(ii)
Percentage of cells with nuclear β-catenin
a
b
a
b
cMaSC
eMaSC
Rat2a/MV7
Rat2a/Wnt1
C (i)
cMaSC
eMaSC
Day 1
Day 4
(ii)
Nucleus
Nucleus
27 px
1 px
(iii)
cMaSC
eMaSC
Percentage out of total paerticles
****
****
Particle size
Day 1
Day 4
(iv)
Mean flouresence intensity
****
****
Day
1
4
1
4
cMaSC
eMaSC

and 4 of culture (Fig. 5*C*, *panel i*) and particle size distribution was analyzed, using a previously established approach (32, 33) (Fig. 5*C*, *panel ii*). In cMaSCs, the percentage of small particles was significantly increased from day 1 to day 4, whereas the percentage of large particles was decreased (Fig. 5*C*, *panel iii*). In eMaSCs, however, no changes in the percentage of small and large particles between days 1 and 4 was observed (Fig. 5*C*, *panel iii*). GSK3$\beta$ expression was also evaluated by analyzing the overall staining intensity in cells and was found to increase over time in cultured cMaSCs but not eMaSCs (Fig. 5*C*, *panel iv*). Collectively, these data suggest that Wnt/$\beta$-catenin signaling is inherently more active in eMaSCs than in cMaSCs.

*Wnt/β-Catenin Signaling Stimulates Growth of eMaSCs in Mammospheres*—To investigate the link between active Wnt/$\beta$-catenin signaling in eMaSCs and their unlimited self-renewal properties in mammosphere cultures, we treated eMaSCs with recombinant Wnt3a (rWnt3a) protein, or the small molecule Wnt inhibitors iCRT3 and salinomycin, and evaluated their mammosphere formation capacity (16, 23, 34). Treatment of eMaSC cultures with rWnt3a was able to significantly increase the number of mammospheres, whereas treatment with iCRT3 and salinomycin significantly reduced mammosphere number (Fig. 6, *A* and *B*). When evaluating how these treatments influenced the size of mammospheres, an increased size with rWnt3a and decreased size with iCRT3 and salinomycin was observed, although this only reached significance for salinomycin (Fig. 6, *C* and *D*). The ability of the rWnt3a and Wnt inhibitors to activate or inhibit Wnt signaling in eMaSCs was confirmed by performing Wnt reporter assays and Western blotting analyses of active $\beta$-catenin in eMaSCs (Fig. 6, *E* and *F*).

*eMaSC-derived MVs Are Stable Inducers of Wnt/β-Catenin Signaling in cMaSCs and Can Rescue the Growth Potential of cMaSCs in Mammospheres*—Having demonstrated the importance of Wnt/$\beta$-catenin signaling for growth of eMaSCs in mammosphere cultures, we wished to know whether this was also the case for MV-mediated Wnt signaling. Specifically, we asked (i) whether eMaSC-MVs, which contain Wnt1 and Wnt3a, can induce Wnt signaling in cMaSCs and (ii) whether cMaSC-MVs, which contain little Wnt1 and Wnt3a but clearly express the Wnt antagonist protein Dkk1, can inhibit Wnt signaling in eMaSCs. In the first set of experiments, we applied MVs isolated from either eMaSCs and cMaSCs to 293T cells transfected with a TCF/LEF-responsive luciferase reporter. We found that eMaSC-MVs, in contrast to cMaSC-MVs, were able to significantly increase luciferase activity in the transfected 293T cells (Fig. 7*A*). These data suggest that MVs from eMaSCs, and not cMaSCs, are capable of activating Wnt signaling in recipient cells. Moreover, and despite the presence of high levels of the Wnt inhibitor Dkk1 in MVs from cMaSCs, no functional inhibitory effect on Wnt signaling was observed in 293T cells exposed to cMaSC MVs (Fig. 7*A*). The latter is interesting because no study has reported to date on the effects in target cells of Wnt inhibitors present in EVs (21). To then study the induction of Wnt signaling mediated by eMaSC-MVs in more detail, experiments were performed in which cMaSCs were treated with either eMaSC-MVs or recombinant Wnt protein 3a (rWnt3a). When evaluating the levels of ABC in these cells, we observed detectable amounts of ABC in cMaSCs that were treated with either eMaSC-MVs or rWnt3a (Fig. 7*B*). Furthermore, the induction of ABC in cMaSCs initiated by eMaSC-MVs could be reduced by both iCRT3 and a specific Wnt3a antibody but not by Dkk1 (Fig. 7*C*). Together, these data suggest that Wnt3a, but not Dkk1, plays an important role in MV-mediated Wnt/$\beta$-catenin signaling.

We next asked whether the packaging of Wnt proteins in MVs has a modulatory effect on the induction of active Wnt signaling. Thus, we treated cMaSCs with eMaSC-MVs or rWnt3a and evaluated the levels of ABC expression in these treated cMaSCs over time. Interestingly, we observed that eMaSC-MVs were able to induce activation of $\beta$-catenin in cMaSCs up to 24 h post-treatment, whereas no ABC could be detected in cells treated with rWnt3a at this point (Fig. 7*D*). A combination of Western blotting analyses, in combination with an equine-specific ELISA, revealed that ~15-fold more rWnt3 was used in these experiments, compared with the amount of Wnt3a expressed in the eMaSC-MVs (Fig. 7, *E* and *F*). Nevertheless, the MVs had a more prolonged effect on the induction of ABC (Fig. 7*D*).

Finally, we investigated the functional consequences of eMaSC-MV-mediated Wnt/$\beta$-catenin signaling on the self-renewal potential of cMaSCs. To this end, mammosphere formation assays were initiated using high passage cMaSCs in the presence or absence of eMaSC-MVs. Interestingly, incubation of high passage cMaSCs with eMaSC-MVs increased the number of mammospheres, an effect comparable with that achieved by rWnt3a treatment (Fig. 8*A*). Furthermore, we found that this effect was significantly reduced by iCRT3, anti-Wnt3a antibody treatment, and the porcupine inhibitor LGK974 but not by Dkk1 (Fig. 8*B*). In addition, we analyzed mRNA expression levels of the mammary stem cell markers heat shock protein family A (Hsp70) member 5 (HSPA5) (35, 36) and leucine-rich repeat containing G protein-coupled receptor 5 (Lgr5) (37) in cMaSCs treated with eMaSC-MV. No significant difference was observed in HSP5A and Lgr5 expression in eMaSC-MV-treated

FIGURE 5. **eMaSCs have inherently more active Wnt/$\beta$-catenin signaling compared with cMaSCs.** *A*, whole cell lysates were immunoblotted as indicated. ABC and p-Dvl-2 were detected in both low and high passage eMaSCs, whereas these proteins were only detected in low passage cMaSCs. Western blot images of three independent experiments were quantified using the Bio-Rad ChemiDoc MP system (*panel ii*), and a representative Western blot image is shown (*panel i*; $n = 3$). *B*, *panel i*, representative fluorescent microscopy of nuclear $\beta$-catenin expression in eMaSCs, which is similar to expression in Rat2/Wnt1 cells, and cMaSCs, which is similar to expression in control Rat2/MV7 cells. *Scale bar*, 25 $\mu$m. *Panel ii*, the percentage of cells with nuclear $\beta$-catenin expression was quantified by analyzing random fields containing at least 100 cells. *C*, *panel i*, representative fluorescent microscopy images of GSK-3$\beta$ expression in eMaSCs and cMaSCs on days 1 and 4 in culture. *Scale bars*, 20 $\mu$m. *Panel ii*, schematic representation of the particle size distribution analyses of GSK3$\beta$ in immunostained cells. *Left panel*, part of an original immunofluorescent image. *Right panel*, image adjustment performed in ImageJ used to define the fluorescent particles software (detailed under "Experimental Procedures"). *Inset/bottom panel*, enlarged part of image, highlighting examples of two particles (*red*) and their size, as measured by ImageJ software. *Panel iii*, quantitation of particle size distribution in GSK3$\beta$-stained cells, comparing the percentage of small (particle size 1) *versus* large (particle size 2–99) fluorescent particles in cMaSCs and eMaSCs between days 1 and 4 in culture ($n = 3$). ****, $p < 0.001$. *Panel iv*, quantitation of overall fluorescence intensity in GSK3$\beta$-stained cMaSCs and eMaSCs on days 1 and 4 in culture ($n = 3$). ****, $p < 0.001$.

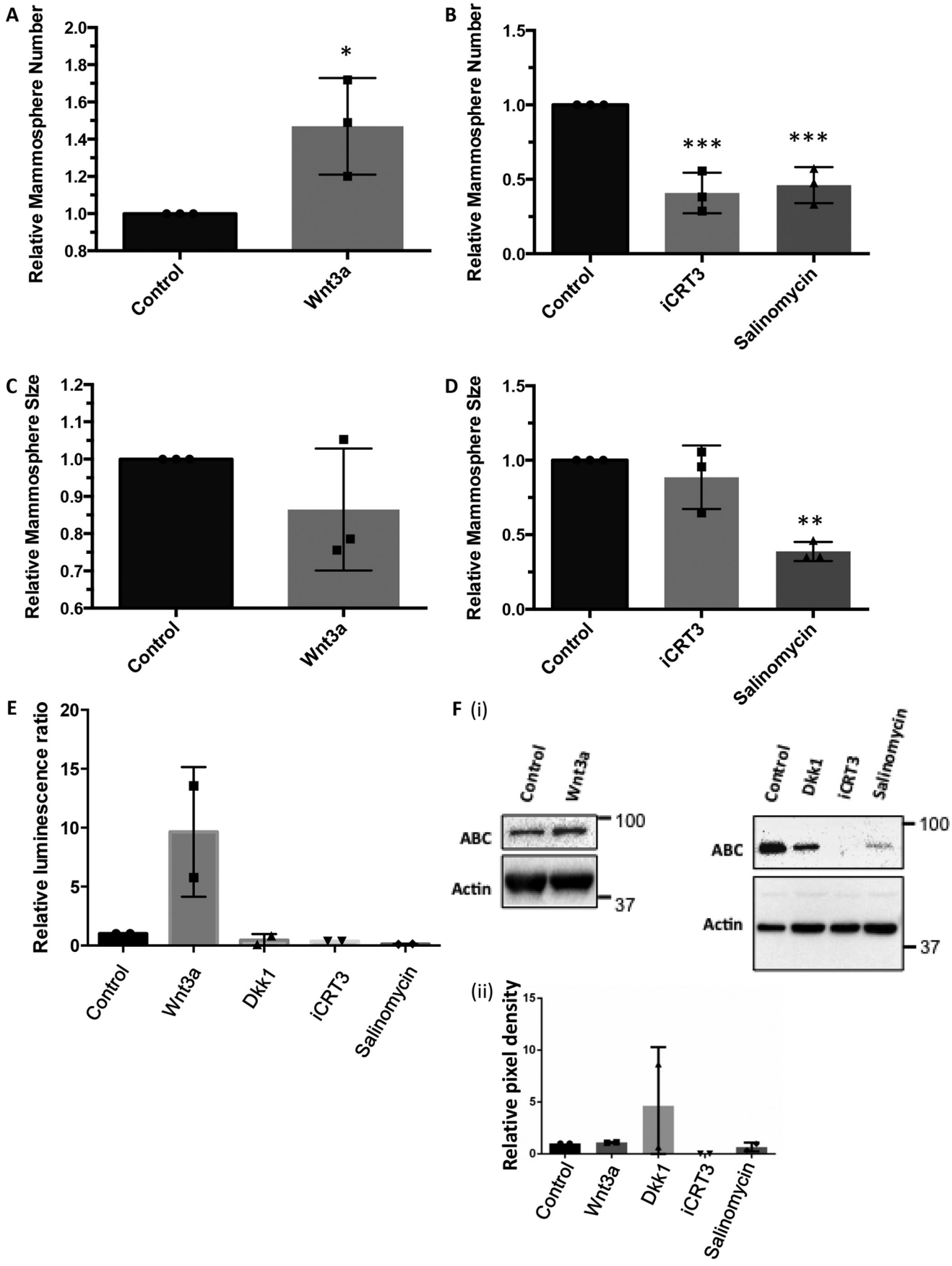
A
Relative Mammosphere Number
2.0
1.8
1.6
1.4
1.2
1.0
0.8
*
Control
Wnt3a
B
Relative Mammosphere Number
1.5
1.0
0.5
0.0
***
***
Control
iCRT3
Salinomycin
C
Relative Mammosphere Size
1.2
1.1
1.0
0.9
0.8
0.7
0.6
Control
Wnt3a
D
Relative Mammosphere Size
1.5
1.0
0.5
0.0
**
Control
iCRT3
Salinomycin
E
Relative luminescence ratio
20
15
10
5
0
Control
Wnt3a
Dkk1
iCRT3
Salinomycin
F (i)
Control
Wnt3a
ABC
Actin
100
37
Control
Dkk1
iCRT3
Salinomycin
ABC
Actin
100
37
(ii)
Relative pixel density
15
10
5
0
Control
Wnt3a
Dkk1
iCRT3
Salinomycin

cMaSCs when compared with cMaSCs incubated with the flowthrough eMaSC CM (control) (Fig. 8*C*). Taken together, these data clearly indicate that eMaSC-MVs are able to restore the growth potential of high passage cMaSCs in mammosphere cultures and that this is dependent, at least in part, on Wnt3a and the activation of Wnt/β-catenin signaling.

## Discussion

This is the first report providing evidence that (i) primary MaSCs release MVs and that these MVs are important mediators in the communication of self-renewal signals. Although secretion of EVs by primary human MaSCs grown as mammospheres has been described previously, that study only focused on EVs smaller than 0.2 μm (*i.e.* exosomes) (24). Here, we describe the secretion of MVs, larger vesicles of ~0.2–2 μm in size, from both equine and canine MaSCs. eMaSCs maintain their growth capacity *in vitro* for an indefinite period, whereas cMaSCs rapidly lose their growth capacity in long term culture. We compared these MaSC-derived MV populations to investigate the underlying mechanism(s) for this strikingly different growth capacity. The data in our present study provide strong evidence that MVs represent a novel mechanism through which MaSCs communicate to promote self-renewal and that this occurs, at least in part, via Wnt3a and the activation of Wnt/β-catenin signaling.

We found that Wnt3a and Wnt1, two ligands that activate the Wnt/β-catenin signaling pathway, showed higher expression in eMaSC-MVs compared with cMaSC-MVs. Importantly, we found that eMaSC-MVs could induce Wnt signaling in late passage cMaSCs and significantly enhance their growth as mammospheres. Stimulation of Wnt signaling via EVs has previously been reported in *Drosophila* cell lines and human cancer cell lines (17, 38–41). Our study is the first to show that a similar MV-mediated mechanism also occurs specifically in MaSCs with unlimited self-renewal properties.

To study in more detail which Wnt activator ligands were specifically important for MV-mediated Wnt signaling induction, we added rWnt3a, eMaSC-MVs, or control medium to high passage cMaSCs and studied the expression of ABC by Western blotting. We observed that Wnt/β-catenin signaling in cMaSCs induced by eMaSC-MVs treatment could be mimicked by rWnt3a. A more direct link between the presence of Wnt-related proteins in MVs and the induction of active Wnt signaling in MaSCs after MVs treatment was provided by showing (i) inhibition of ABC expression and (ii) significant reduction of mammosphere numbers when eMaSC-MVs culturing was performed in the presence of anti-Wnt3a antibodies. The involvement of MV-associated Wnt3a in self-renewal and growth capacity of stem cells has been proposed previously (42), where Wnt3 proteins were detected in the MVs of ES cells. Our current study now provides strong evidence that Wnt3a signaling via MVs is indeed an important physiological mechanism for stem cell renewal and growth.

During our studies, a few surprising observations were made when using inhibitors of the Wnt signaling pathway. First, we found that treatment of our cells with iCRT3, an inhibitor of Wnt signaling by regulating β-catenin-TCF interactions, resulted in a strong reduction of ABC (Figs. 6 and 7). This is in contrast to previous literature, where it was demonstrated that iCRT3 inhibits Wnt signaling by antagonizing the transcriptional function of nuclear β-catenin while not affecting its cytoskeletal function in stabilizing adherent junctions at the cell membrane (43). Second, we could not observe any suppressive effect of Dkk1 in regulating ABC expression nor in regulating mammosphere numbers when cMaSCs were exposed to eMaSC-MV in the presence of Dkk1 (Fig. 7). This was not due to a lack of Dkk1 activity, because we observed a clear inhibitory effect in our inducible TCF/LEF-responsive firefly luciferase assay. Although rather unlikely because of the extreme conservation of Wnt signaling components within *mammalia*, one plausible explanation for these contradictory observations made in our study could be a species difference. Experimental information on Wnt signaling in species like dogs and horses is rather scarce and so future experiments focused on studying this pathway in these species in greater depth might shed more light into similarities and differences in canonical Wnt signaling among different mammalian species.

The majority of available data on signal pathways that regulate growth and self-renewal of MaSCs comes from rodents (1). Indeed, rodents have played an indispensable and pivotal role in the study of MaSC physiology, and this animal species will keep on being a major research resource (1). However, an important bottleneck of using only one model species is that some key insights might be lost because of the absence of variation in regard to physiological functioning of the mammary gland (22). In this study, we attempted to overcome this by comparing MaSCs from two different species, namely dogs and horses, whose MaSCs showed a strikingly different phenotype in long term *in vitro* cultures. Taking advantage of this difference permitted us to elucidate a novel mechanism, highlighting the importance of comparative physiology to study basic physiological mechanisms. One of the questions raised by this study is why the canine and equine MaSCs display such different phenotypes in their growth and self-renewal capacities. Although speculative at this point, we hypothesize that the answer to this question might be found in the supportive role of the mammary gland niche surrounding MaSCs *in vivo*. It is possible that

FIGURE 6. **Active Wnt/β-catenin signaling stimulates growth of eMaSCs in mammospheres.** Secondary mammospheres of eMaSCs were counted and measured 1 week after plating dissociated cells and treated as indicated on ultra low attachment plates ($n = 3$). *, $p < 0.05$; **, $p < 0.01$; ***, $p < 0.005$. *A*, increased mammosphere formation in eMaSC cultures treated with Wnt3a *versus* control. *B*, decreased mammosphere formation in eMaSC cultures treated with iCRT3 and salinomycin *versus* control. *C*, no significant increase in mammosphere size in eMaSC cultures treated with Wnt3a *versus* control. *D*, only treatment of eMaSCs with salinomycin resulted in a significant decrease in mammosphere size. *E*, HEKT cells, transfected for 24 h with a mixture of inducible TCF/LEF-responsive firefly luciferase and constitutively expressing *Renilla* luciferase constructs, were treated with Wnt3a, iCRT3, salinomycin, Dkk1, or control medium. Significant up-regulation and down-regulation of Wnt signaling activity was detected after Wnt3a and iCRT3/salinomycin/Dkk1treatment, respectively ($n = 2$). *, $p < 0.05$; **, $p < 0.01$. *F*, eMaSC lysates treated with Wnt3a, iCRT3, salinomycin, Dkk1, or control medium were immunoblotted for ABC and β-actin loading control. Western blot images of two independent experiments were quantified using the Bio-Rad ChemiDoc MP system (*panel ii*), and a representative Western blot image is shown (*panel i*).

cMaSCs are more dependent on paracrine signals from other cell types present in the mammary gland niche, whereas eMaSCs are more self-sufficient and provide autocrine signals to ensure proper self-renewal. Consequently, removing MaSCs from their natural environment, as when culturing these cells *in vitro*, allows eMaScs to survive in long term *in vitro* cultures,

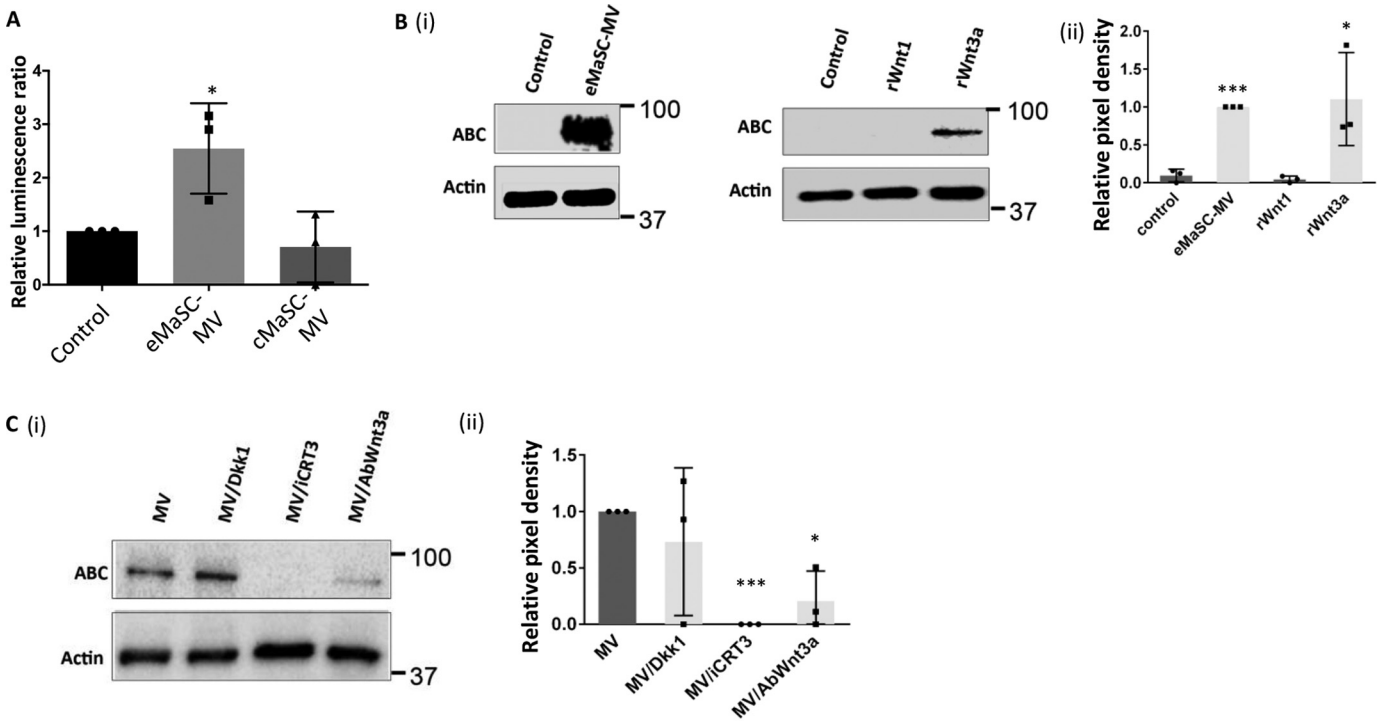


| | Concentration | | | Optical Density |
|---|---|---|---|---|
| | X | Upper Limit | Lower Limit | Y |
| eMaSC-MV | 12.979 | 19.638 | 5.680 | 0.056 |
| rWnt3a | 143.891 | 153.283 | 135.589 | 0.853 |

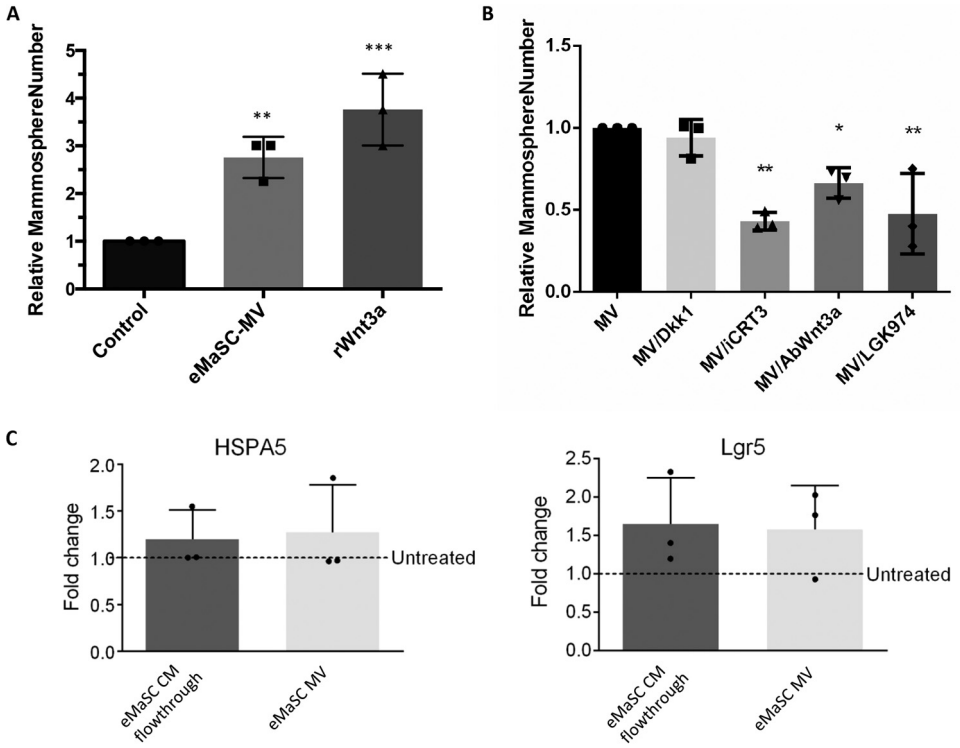


FIGURE 8. **eMaSC-MVs can rescue growth of cMaSCs in mammospheres.** Secondary mammospheres of cMaSCs were measured and counted 1 week after plating dissociated cells, treated as indicated, on ultra low attachment plates ($n = 3$). *, $p < 0.05$; **, $p < 0.01$; ***, $p < 0.005$). *A*, increased mammosphere formation in cMaSC cultures treated with eMaSC-MV or 200 ng/ml Wnt3a *versus* control. *B*, decreased mammosphere formation in eMaSC-MV-treated cMaSC cultures after treatment with iCRT3, anti-Wnt3a antibody, or LGK974 but not Dkk1s *versus* control. *C*, mRNA expression levels of the mammary stem cell markers HSPA5 and Lgr5 in cMaSCs treated with eMaSC-MV or eMaSC CM flowthrough (control), expressed as fold change relative to untreated cMaSCs ($n = 3$).

whereas cMaSCs lose their self-renewal capacities because of the lack of signals from the microenvironment. Studies comparing the mammary stem cell niche in these different species will be necessary to confirm or refute this hypothesis.

## Experimental Procedures

*Cell Culture*—MaSCs were isolated from equine and canine mammary gland tissues and characterized as previously described (44). MaSCs were maintained in EpSC medium consisting of DMEM/Ham's F-12 (50/50) supplemented with 10% of FBS, 2% B27 (all from Invitrogen), 1% penicillin/streptomycin/antimycotic (Sigma), 10 ng/ml basic fibroblast growth factor (BioVision), and 10 ng/ml epidermal growth factor (Sigma). Hek293T cells were purchased from ATCC and were maintained in culture medium consisting of DMEM supplemented with 10% FBS and 1% penicillin/streptomycin. Control (Rat2/MV7) and Wnt-1 expressing Rat-2a (Rat2/Wnt1) cells, from which the generation was reported previously (45), were maintained in culture medium consisting of DMEM supplemented with 10% FBS and 1% penicillin/streptomycin.

*PDT and Mammosphere Cultures*—PDT was calculated using the following formula: PDT = cell culture time/($\ln(N_f/N_i)/\ln 2$), where $N_f$ is the final number of cells, and $N_i$ is the initial number of cells. Mammosphere cultures were initiated as described before (44). First generation mammospheres, which developed from mammary gland tissue-derived cells on ultralow attachment plates (Corning), were maintained in culture for 11 days. At day 11 post-seeding, all mammospheres were collected and plated on adhesive tissue culture dishes in MaSC medium. To obtain second generation mammospheres, single cells were replated on ultralow attachment plates at a density of 1000 cells/ml, as previously described (44, 46). After 7 days, 20 random fields of mammospheres per condition were photographed. To calculate the mammosphere forming efficiency, the number of mammospheres was divided by the original number of single cells seeded and expressed as a percent-

FIGURE 7. **eMaSC-MVs are stable inducers of Wnt/β-catenin signaling in cMaSCs.** *A*, HEKT cells transfected for 24 h with a mixture of inducible TCF/LEF-responsive firefly luciferase and constitutively expressing *Renilla* luciferase constructs were treated with either eMaSC-MV, cMaSC-MV, or control medium. A significant up-regulation of Wnt signaling activity was detected after treatment with eMaSC-MV ($n = 3$). *, $p < 0.05$. Next, cMaSC lysates were immunoblotted for ABC and β-actin loading control. Representative Western blots of three independent experiments are shown. *B*, induction of ABC expression in cMaSCs treated with eMaSC-MV and rWnt3a. Western blot images of three independent experiments were quantified using the Bio-Rad ChemiDoc MP system (*panel ii*), and a representative Western blot image is shown (*panel i*; $n = 3$). *, $p < 0.05$; ***, $p < 0.0005$. *C*, decreased ABC expression in eMaSC-MV-treated cMaSCs after iCRT3 and anti-Wnt3a antibody but not Dkk1 treatment. Western blot images of three independent experiments were quantified using the Bio-Rad ChemiDoc MP system (*panel ii*), and a representative Western blot image is shown (*panel i*; $n = 3$). *, $p < 0.05$; ***, $p < 0.0005$. *D*, ABC expression is still detectable at 24 h in cMaSCs treated with eMaSC-MVs but not rWnt3a. Western blot images of three independent experiments were quantified using the Bio-Rad ChemiDoc MP system (*panel ii*), and a representative Western blot image is shown (*panel i*; $n = 3$). *, $p < 0.05$. *E*, eMaSC-MVs lysates and 200 ng/ml rWFnt3a were immunoblotted for Wnt3a. A representative Western blot image is shown of three independent experiments ($n = 3$). *F*, Wnt3a concentration was quantified in eMaSC-MVs and rWnt3a using an equine-specific Wnt3a ELISA. Absorbance was measured at 450 nm on a Multiskan EX microplate reader using Ascent software from Thermo Scientific ($n = 3$).

age, exactly as previously described (44, 46). Mammosphere sizes were determined using ImageJ software. All experiments were performed in triplicate.

*Collection of CM, Isolation of MVs, and Vesicle Size Determination*—T75 flasks were seeded with $6 \times 10^5$ MaSCs in 8 ml of expansion medium. After 48 h, CM was collected, centrifuged twice for 10 min at $300 \times g$ to remove intact cells, and then used for further experiments directly or to isolate MVs. Intact MVs were isolated as previously described (47), with some modifications. For each of the MVs preparation, eight T75 flasks of MaSCs ($\sim 2.4 \times 10^7$ cells) were rinsed several times with PBS and incubated in serum-free EpSC medium overnight. CM was removed from these cells and centrifuged at $300 \times g$ for 10 min to pellet intact cells and again at $3{,}000 \times g$ for 20 min to remove cell debris. This partially clarified CM was then filtered through a 0.22-$\mu$m Steriflip filter unit and washed with 10 ml of PBS. If being used for biological assays, MVs retained by the filter were resuspended in 300 $\mu$l of EpSC medium. However, if used to generate lysates, MVs were lysed in radioimmune precipitation assay buffer containing 20 mM Tris (pH 8.0), 137 mM NaCl, 10% glycerol, 1% Nonidet P-40, 0.1% SDS, 0.5% deoxycholate, 0.2 mM PMSF, and 1× general protease inhibitor. Size determination of EVs, including MVs, in MaSC CM was performed using a Zetasizer Nano ZS (Malvern Instruments) according to the manufacturer's instructions.

*Recombinant Proteins, Plasmids, and Small Molecules*—The PM-GFP vector was a gift from Tobias Meyer, Stanford University (Addgene, plasmid no. 21213). Recombinant (r)Wnt3a and rDkk1 were from R & D Systems and used at a concentration of 200 ng/ml. The small molecule inhibitors iCRT3 (Calbiochem; a selective CRT $\beta$-catenin-responsive transcription inhibitor), salinomycin (Sigma; an antibiotic potassium ionophore that inhibits proximal Wnt signaling by interfering with LPR6 phosphorylation), and LGK974 (Cayman Chemicals; a specific small molecule porcupine inhibitor that reduces Wnt secretion) were used at 25 mM, 10 mM, and 1 $\mu$M, respectively.

*Antibodies*—For immunoblotting, the following primary antibodies were used: anti-flotillin-2 (Cell Signaling, catalog no. 3436, 1:1000) (47), anti-RhoA (Cell Signaling, catalog no. 2117, 1:1000) (47), anti-ABC (Millipore, catalog no. 05-665, 0.5 $\mu$g/ml) (48), anti-Dishevelled-2 (Dvl2) (Cell Signaling, catalog no. 3216, 1:1000) (57), anti-Wnt1 (R & D Systems, catalog no. AF1620, 1:1000) (49), anti-Wnt3a (R & D Systems, catalog no. MAB1324, 2 $\mu$g/ml) (50), anti-Wnt5a (R & D Systems, catalog no. AF645, 1 $\mu$g/ml) (51), anti-Dkk1 (Abcam, catalog no. 109416, 1:1000) (52), and anti-$\beta$-actin (Abcam, catalog no. 8227, 1:5000) (53). For immunofluorescence, the following primary antibodies were used: $\beta$-catenin (BD Biosciences, catalog no. 610153, 1:500) (54) or GSK3$\beta$ (Abcam, catalog no. 32391, 1:200) (55) antibodies. For flow cytometry, the following primary antibodies were used: anti-flotillin-2 (Cell Signaling, catalog no. 3436, 1:50) (47) and anti-CD81 (Santa Cruz, catalog no. 9158, 1:50) (56). In all antibody assays, commercially available antibodies were used in the presence of isotype controls. For the rat anti-Wnt3a antibody, human recombinant Wnt3a protein (R & D Systems) was used as a positive control. For the mouse anti-$\beta$-catenin antibody, Rat2/Wnt1 cells were used as a positive control.

*Immunoblot Analyses*—Cells and microvesicles were lysed in radioimmune precipitation assay buffer containing 20 mM Tris (pH 8.0), 137 mM NaCl, 10% glycerol, 1% Nonidet P-40, 0.1% SDS, 0.5% deoxycholate, 0.2 mM PMSF, and 1× general protease inhibitor. The protein concentrations of whole cell lysates were determined using the Thermo Fisher BCA assay, and 10 $\mu$g of protein was loaded per lane. For MV, an average of 5 $\mu$g of protein was loaded per lane. 6× sample buffer (300 mM Tris-HCl, pH 6.8, 60% glycerol, 30 mM DTT, 6% SDS) was added to yield a final concentration of 1×, and lysates were boiled at 95 °C for 10 min. Samples were subjected to SDS/PAGE and transferred to Immobilin PVDF membranes (Millipore) using a transblot turbo system (Bio-Rad). The membranes were blocked in 5% BSA diluted in TBS. The following primary antibodies were incubated overnight at 4 °C: anti-flotillin-2 (Cell Signaling), anti-RhoA (Cell Signaling), anti-ABC (Millipore), anti-Dvl2 (Cell Signaling), anti-Wnt1 (R & D Systems), anti-Wnt3a (R & D Systems), anti-Wnt5a (R & D Systems), anti-Dkk1 (Abcam), and anti-$\beta$-actin (Abcam, loading control). The blots were washed and then incubated with secondary antibodies for 1 h at room temperature. The blots were washed for 50 min (10 × 5 min) with TBS-Tween and visualized by chemiluminescence using Clarity Western ECL (Bio-Rad). The gels were imaged on a Bio-Rad ChemiDoc MP system (Bio-Rad), and the band intensities were determined using Image Lab software. Intensities of the bands of interest were divided by the intensities of loading control bands to calculate relative band intensity. Western blots from at least three independent experiments were performed per analysis.

*Immunofluorescence*—To visualize EVs, the cells were incubated with 5 $\mu$g/ml FM® 1–43FX plasma membrane dye (Life Technologies) diluted in PBS for 1 min, fixed in ice-cold 4% formaldehyde, and rinsed three times with PBS before being analyzed by fluorescence microscopy. To visualize $\beta$-catenin and GSK3$\beta$, the cells were treated with 4% formaldehyde, permeabilized with 0.1% or 0.5% Triton X-100, and then blocked with 10% BSA. The cells were incubated with $\beta$-catenin (BD Biosciences) or GSK3$\beta$ (Abcam) antibodies, washed with 1% BSA in PBS, and incubated with a 488-conjugated secondary antibody (Jackson) and DAPI (Sigma) to label nuclei. For image analyses of GSK3$\beta$, 10 random images were taken of each group using the 40× objective of a confocal laser scanning microscope (Zeiss, Oberkochen, Germany), and the distribution of particle size was analyzed using ImageJ software (National Institute of Health, Bethesda, Maryland), as previously described (32, 33). Briefly, the upper threshold was set at 100 to exclude the blue (DAPI), and brightness lower threshold was set at 50. The particle size analyses were performed automatically by the software, with the definition of particle circularity set between 0.00 and 1.00 and results not filtered for particle size (0-infinity). All counted particles were recorded, and their size distribution was calculated. To determine cargo transfer from eMaSC-MVs to cMaSCs, cMaSCs were incubated with MVs from PM-GFP transfected eMaSCs and visualized 2 h later. All cell images (with exception of the GSK3$\beta$ experiments) were captured and processed using an Eclipse TE2000-U inverted fluorescence microscope (Nikon), and image analyses and quantitation was performed in a blinded manner.

**TABLE 1**
**Primers used in this study**

| Gene | Forward primer (5′ → 3′) | Reverse primer (5′ → 3′) |
|---|---|---|
| GAPDH (glyceraldehyde 3-phosphate dehydrogenase) | ACACCCACTCTTCCACCTTC | TACTCCTTGGAGGCCATGTG |
| Lgr5 (leucine-rich repeat containing G protein-coupled receptor 5) | TTTGCTGGCCTTCACAGTC | ACTGAAGGCTTCGCAGGTT |
| HSPA5 (heat shock protein family A (Hsp70) member 5) | ACTGCGGAGGCTTATTTGG | TTGGGCATCATTGAAGTAGG |

*Flow Cytometry*—For the immunophenotyping of putative MVs, vesicles were incubated with 4 $\mu$m, 4% aldehyde/sulfate latex beads (Invitrogen) for 15 min at room temperature, and 3.33× total volume of PBS was added to the mixture for an additional 2.5 h at room temperature while stirring. To stop the reaction, 1 M glycine was added for 30 min at room temperature. The beads were centrifuged at 1000 × *g* for 3 min, washed with PBS, and incubated with primary antibodies against flotillin-2 (Cell Signaling) and CD81 (Santa Cruz), or isotype controls, for 1 h at room temperature. The beads were washed, incubated with a 488-conjugated secondary antibody (Jackson) for 30 min, rinsed in PBS, and analyzed using KALUZA software.

*Mass Spectrometry*—MVs lysates were trypsin-digested and resulting peptide fragments were analyzed using an Orbitrap Velos on-line LC/MS/MS system (Applied Biosystems/MDS Sciex). The MS/MS raw data files were submitted to Mascot 2.2 (Matrix Science) for NCBI database searching, and the results were further analyzed using PANTHER software.

*TCF/LEF-responsive Luciferase Assay*—HEK293T cells were seeded in 96-well plates at a density of $1 \times 10^4$ cells and transfected, using FuGENE HD (Roche Molecular Biochemicals), 24 h after seeding with 100 ng of TCF/LEF reporter plasmid consisting of a mixture of inducible TCF/LEF-responsive firefly luciferase and constitutively expressing *Renilla* luciferase constructs (40:1) (Qiagen). Negative control plasmid, consisting of a mixture of non-inducible firefly luciferase construct and constitutively expressing *Renilla* luciferase construct (40:1), and positive control plasmid, consisting of a mixture of constitutively expressing GFP, constitutively expressing firefly luciferase, and constitutively expressing *Renilla* luciferase constructs (40:1:1), were included also. After 20 h of transfection, medium was changed, and 4 h later, the cells were either treated with MV, recombinant proteins, or small molecule inhibitors. Luciferase gene expression was measured 16 h later using a Dual-Glo luciferase assay kit (Promega). Luciferase activity was normalized to *Renilla* luciferase activity, and all experiments were performed in duplicate and at least three times.

*Wnt3a ELISA*—To detect the presence of Wnt3a in eMaSC-MVs, an equine-specific Wnt3a ELISA kit was used according to the manufacturer's instructions (MyBiosource). The resulting yellow color was read at 450 nm on a Multiskan EX microplate reader using Ascent software (Thermo Scientific). rWnt3a was included as a control.

*Gene Expression Analyses*—cMaSCs were treated with eMaSC-MV, and 24 h later, mRNA was extracted from these cells using an RNeasy Plus Mini Kit according to the manufacturer's instructions (Qiagen). mRNA from control cells consisting of untreated cMaSCs or cMaSCs treated with the eMaSC CM after passing the 0.22-$\mu$m filter were also included (flowthrough). cDNA was synthesized using M-MLV reverse transcriptase (USB, Cleveland, OH) and SYBR green-based quantitative PCR assays were carried out on an Applied Biosystems 7500 Fast Real-Time PCR instrument (Applied Biosystems) to determine fold changes of genes of interest. The comparative threshold cycle (*Ct*) method ($2^{-\Delta\Delta Ct}$) was used to quantify gene expression levels in which $\Delta\Delta Ct = \Delta Ct(\text{sample}) - \Delta Ct$ (reference). The reference gene was glyceraldehyde-3-phosphate dehydrogenase (GAPDH). Primer sequences are listed in Table 1. All samples were run in triplicate.

*Statistical Analyses*—All numerical data are presented as means ± standard deviation of at least three independent experiments. Statistical analysis was performed using Microsoft Excel and GraphPad Prism. The data sets with two groups were subjected to a two-tailed, unpaired Student's *t* test.

*Author Contributions*—The study was designed by L. B., M. A., G. R., A. M. C. B., R. A. C., and G. R. V. d. W. Experiments were conducted by L. B., B. S., G. R., and M. M. The data were analyzed by L. B., M. A., G. R., and G. R. V. d. W. The manuscript was written by L. B., M. A., G. R., A. M. C. B., R. A. C., and G. R. V. d. W. This work was supervised by G. R. V. d. W.

*Acknowledgments—We gratefully acknowledge the Cornell Proteomics Core Facility staff, Bridget Kreger and Allison Seebald for their excellent technical support, and Christian Burvenich for fruitful discussions on Comparative Physiology.*

**References**

1. Liu, S., Dontu, G., and Wicha, M. S. (2005) Mammary stem cells, self-renewal pathways, and carcinogenesis. *Breast Cancer Res.* **7,** 86–95
2. Ercan, C., van Diest, P. J., and Vooijs, M. (2011) Mammary development and breast cancer: the role of stem cells. *Curr. Mol. Med.* **11,** 270–285
3. Dey, D., Saxena, M., Paranjape, A. N., Krishnan, V., Giraddi, R., Kumar, M. V., Mukherjee, G., and Rangarajan, A. (2009) Phenotypic and functional characterization of human mammary stem/progenitor cells in long term culture. *PLoS One* **4,** e5329
4. Boulanger, C. A., Wagner, K.-U., and Smith, G. H. (2005) Parity-induced mouse mammary epithelial cells are pluripotent, self-renewing and sensitive to TGF-$\beta$1 expression. *Oncogene* **24,** 552–560
5. Brennan, K. R., and Brown, A. M. (2004) Wnt proteins in mammary development and cancer. *J. Mammary Gland Biol. Neoplasia* **9,** 119–131
6. Dontu, G., Jackson, K. W., McNicholas, E., Kawamura, M. J., Abdallah, W. M., and Wicha, M. S. (2004) Role of Notch signaling in cell-fate determination of human mammary stem/progenitor cells. *Breast Cancer Res.* **6,** R605–R615
7. Ingham, P. W., and McMahon, A. P. (2001) Hedgehog signaling in animal development: paradigms and principles. *Genes Dev.* **15,** 3059–3087
8. Leung, C., Lingbeek, M., Shakhova, O., Liu, J., Tanger, E., Saremaslani, P., Van Lohuizen, M., and Marino, S. (2004) Bmi1 is essential for cerebellar development and is overexpressed in human medulloblastomas. *Nature* **428,** 337–341
9. Lewis, M. T., Ross, S., Strickland, P. A., Sugnet, C. W., Jimenez, E., Hui, C., and Daniel, C. W. (2001) The Gli2 transcription factor is required for normal mouse mammary gland development. *Dev. Biol.* **238,** 133–144

10. Molofsky, A. V., Pardal, R., and Morrison, S. J. (2004) Diverse mechanisms regulate stem cell self-renewal. *Curr. Opin. Cell Biol.* **16,** 700–707
11. Reya, T., Duncan, A. W., Ailles, L., Domen, J., Scherer, D. C., Willert, K., Hintz, L., Nusse, R., and Weissman, I. L. (2003) A role for Wnt signalling in self-renewal of haematopoietic stem cells. *Nature* **423,** 409–414
12. Stiles, B., Groszer, M., Wang, S., Jiao, J., and Wu, H. (2004) PTENless means more. *Dev. Biol.* **273,** 175–184
13. Zeng, Y. A., and Nusse, R. (2010) Wnt proteins are self-renewal factors for mammary stem cells and promote their long-term expansion in culture. *Cell Stem Cell* **6,** 568–577
14. Komiya, Y., and Habas, R. (2008) Wnt signal transduction pathways. *Organogenesis* **4,** 68–75
15. Park, H. W., Kim, Y. C., Yu, B., Moroishi, T., Mo, J.-S., Plouffe, S. W., Meng, Z., Lin, K. C., Yu, F.-X., Alexander, C. M., Wang, C.-Y., and Guan, K.-L. (2015) Alternative Wnt signaling activates YAP/TAZ. *Cell* **162,** 780–794
16. Many, A. M., and Brown, A. M. (2014) Both canonical and non-canonical Wnt signaling independently promote stem cell growth in mammospheres. *PLoS One* **9,** e101800
17. Gross, J. C., Chaudhary, V., Bartscherer, K., and Boutros, M. (2012) Active Wnt proteins are secreted on exosomes. *Nat. Cell Biol.* **14,** 1036–1045
18. Morrell, N. T., Leucht, P., Zhao, L., Kim, J.-B., ten Berge, D., Ponnusamy, K., Carre, A. L., Dudek, H., Zachlederova, M., McElhaney, M., Brunton, S., Gunzner, J., Callow, M., Polakis, P., Costa, M., *et al.* (2008) Liposomal Packaging Generates Wnt Protein with In Vivo Biological Activity. *PLoS One* **3,** e2930
19. Raposo, G., and Stoorvogel, W. (2013) Extracellular vesicles: exosomes, microvesicles, and friends. *J. Cell Biol.* **200,** 373–383
20. Koch, R., Demant, M., Aung, T., Diering, N., Cicholas, A., Chapuy, B., Wenzel, D., Lahmann, M., Güntsch, A., Kiecke, C., Becker, S., Hupfeld, T., Venkataramani, V., Ziepert, M., Opitz, L., *et al.* (2014) Populational equilibrium through exosome-mediated Wnt signaling in tumor progression of diffuse large B-cell lymphoma. *Blood* **123,** 2189–2198
21. Gangoda, L., Boukouris, S., Liem, M., Kalra, H., and Mathivanan, S. (2015) Extracellular vesicles including exosomes are mediators of signal transduction: are they protective or pathogenic? *Proteomics* **15,** 260–271
22. Borena, B. M., Bussche, L., Burvenich, C., Duchateau, L., and Van de Walle, G. R. (2013) Mammary stem cell research in veterinary science: an update. *Stem Cells Dev.* **22,** 1743–1751
23. Liao, M.-J., Zhang, C. C., Zhou, B., Zimonjic, D. B., Mani, S. A., Kaba, M., Gifford, A., Reinhardt, F., Popescu, N. C., Guo, W., Eaton, E. N., Lodish, H. F., and Weinberg, R. A. (2007) Enrichment of a population of mammary gland cells that form mammospheres and have *in vivo* repopulating activity. *Cancer Res.* **67,** 8131–8138
24. Gonzalez, E., Piva, M., Rodriguez-Suarez, E., Gil, D., Royo, F., Elortza, F., Falcon-Perez, J. M., and Vivanco, M. (2014) Human mammospheres secrete hormone-regulated active extracellular vesicles. *PLoS One* **9,** e83955
25. Staal, F. J., van Noort, M., Strous, G. J., and Clevers, H. C. (2002) Wnt signals are transmitted through N-terminally dephosphorylated β-catenin. *EMBO Rep.* **3,** 63–68
26. Li, V. S., Ng, S. S., Boersema, P. J., Low, T. Y., Karthaus, W. R., Gerlach, J. P., Mohammed, S., Heck, A. J., Maurice, M. M., Mahmoudi, T., and Clevers, H. (2012) Wnt signaling through inhibition of β-catenin degradation in an intact Axin1 complex. *Cell* **149,** 1245–1256
27. Rotherham, M., and El Haj, A. J. (2015) Remote activation of the Wnt/β-catenin signalling pathway using functionalised magnetic particles. *PLoS One* **10,** e0121761
28. Barker, N., and van den Born, M. (2008) Detection of β-catenin localization by immunohistochemistry. *Methods Mol. Biol.* **468,** 91–98
29. Giarré, M., Semënov, M. V., and Brown, A. M. (1998) Wnt signaling stabilizes the dual-function protein β-catenin in diverse cell types. *Ann. N.Y. Acad. Sci.* **857,** 43–55
30. Stamos, J. L., and Weis, W. I. (2013) The β-catenin destruction complex. *Cold Spring Harb. Perspect. Biol.* **5,** a007898
31. Taelman, V. F., Dobrowolski, R., Plouhinec, J. L., Fuentealba, L. C., Vorwald, P. P., Gumper, I., Sabatini, D. D., and De Robertis, E. M. (2010) Wnt signaling requires sequestration of glycogen synthase kinase 3 inside multivesicular endosomes. *Cell* **143,** 1136–1148
32. Demeule, B., Gurny, R., and Arvinte, T. (2007) Detection and characterization of protein aggregates by fluorescence microscopy. *Int. J. Pharm.* **329,** 37–45
33. Lohr, C., Kunding, A. H., Bhatia, V. K., and Stamou, D. (2009) Constructing size distributions of liposomes from single-object fluorescence measurements. *Methods Enzymol.* **465,** 143–160
34. Liu, S., Dontu, G., Mantle, I. D., Patel, S., Ahn, N. S., Jackson, K. W., Suri, P., and Wicha, M. S. (2006) Hedgehog signaling and Bmi-1 regulate self-renewal of normal and malignant human mammary stem cells. *Cancer Res.* **66,** 6063–6071
35. Spike, B. T., Kelber, J. A., Booker, E., Kalathur, M., Rodewald, R., Lipianskaya, J., La, J., He, M., Wright, T., Klemke, R., Wahl, G. M., and Gray, P. C. (2014) CRIPTO/GRP78 signaling maintains fetal and adult mammary stem cells *ex vivo*. *Stem Cell Reports* **2,** 427–439
36. Zhu, G., Wang, M., Spike, B., Gray, P. C., Shen, J., Lee, S.-H., Chen, S.-Y., and Lee, A. S. (2014) Differential requirement of GRP94 and GRP78 in mammary gland development. *Sci. Rep.* **4,** 5390
37. Plaks, V., Brenot, A., Lawson, D. A., Linnemann, J. R., Van Kappel, E. C., Wong, K. C., de Sauvage, F., Klein, O. D., and Werb, Z. (2013) Lgr5-expressing cells are sufficient and necessary for postnatal mammary gland organogenesis. *Cell Rep.* **3,** 70–78
38. Korkut, C., Ataman, B., Ramachandran, P., Ashley, J., Barria, R., Gherbesi, N., and Budnik, V. (2009) Trans-synaptic transmission of vesicular Wnt signals through Evi/Wntless. *Cell* **139,** 393–404
39. Luga, V., Zhang, L., Viloria-Petit, A. M., Ogunjimi, A. A., Inanlou, M. R., Chiu, E., Buchanan, M., Hosein, A. N., Basik, M., and Wrana, J. L. (2012) Exosomes mediate stromal mobilization of autocrine Wnt-PCP signaling in breast cancer cell migration. *Cell* **151,** 1542–1556
40. Koles, K., and Budnik, V. (2012) Exosomes go with the Wnt. *Cell. Logist.* **2,** 169–173
41. Zhang, L., and Wrana, J. L. (2014) The emerging role of exosomes in Wnt secretion and transport. *Curr. Opin. Genet. Dev.* **27,** 14–19
42. Ratajczak, J., Miekus, K., Kucia, M., Zhang, J., Reca, R., Dvorak, P., and Ratajczak, M. Z. (2006) Embryonic stem cell-derived microvesicles reprogram hematopoietic progenitors: evidence for horizontal transfer of mRNA and protein delivery. *Leukemia* **20,** 847–856
43. Gonsalves, F. C., Klein, K., Carson, B. B., Katz, S., Ekas, L. A., Evans, S., Nagourney, R., Cardozo, T., Brown, A. M., and DasGupta, R. (2011) An RNAi-based chemical genetic screen identifies three small-molecule inhibitors of the Wnt/wingless signaling pathway. *Proc. Natl. Acad. Sci. U.S.A.* **108,** 5954–5963
44. Spaas, J. H., Chiers, K., Bussche, L., Burvenich, C., and Van de Walle, G. R. (2012) Stem/progenitor cells in non-lactating versus lactating equine mammary gland. *Stem Cells Dev.* **21,** 3055–3067
45. Jue, S. F., Bradley, R. S., Rudnicki, J. A., Varmus, H. E., and Brown, A. M. (1992) The mouse Wnt-1 gene can act via a paracrine mechanism in transformation of mammary epithelial cells. *Mol. Cell. Biol.* **12,** 321–328
46. Stingl, J., Eirew, P., Ricketson, I., Shackleton, M., Vaillant, F., Choi, D., Li, H. I., and Eaves, C. J. (2006) Purification and unique properties of mammary epithelial stem cells. *Nature* **439,** 993–997
47. Antonyak, M. A., Li, B., Boroughs, L. K., Johnson, J. L., Druso, J. E., Bryant, K. L., Holowka, D. A., and Cerione, R. A. (2011) Cancer cell-derived microvesicles induce transformation by transferring tissue transglutaminase and fibronectin to recipient cells. *Proc. Natl. Acad. Sci. U.S.A.* **108,** 4852–4857
48. Jia, D., Yang, W., Li, L., Liu, H., Tan, Y., Ooi, S., Chi, L., Filion, L. G., Figeys, D., and Wang, L. (2015) β-Catenin and NF-κB co-activation triggered by TLR3 stimulation facilitates stem cell-like phenotypes in breast cancer. *Cell Death Differ.* **22,** 298–310
49. Chong, Z. Z., Shang, Y. C., Hou, J., and Maiese, K. (2010) Wnt1 neuroprotection translates into improved neurological function during oxidant stress and cerebral ischemia through AKT1 and mitochondrial apoptotic pathways. *Oxid. Med. Cell. Longev.* **3,** 153–165
50. Neumann, J., Schaale, K., Farhat, K., Endermann, T., Ulmer, A. J., Ehlers, S., and Reiling, N. (2010) Frizzled1 is a marker of inflammatory macrophages, and its ligand Wnt3a is involved in reprogramming *My-*

*cobacterium tuberculosis*-infected macrophages. *FASEB J.* **24,** 4599–4612

51. Rauner, M., Stein, N., Winzer, M., Goettsch, C., Zwerina, J., Schett, G., Distler, J. H., Albers, J., Schulze, J., Schinke, T., Bornhäuser, M., Platzbecker, U., and Hofbauer, L. C. (2012) WNT5A is induced by inflammatory mediators in bone marrow stromal cells and regulates cytokine and chemokine production. *J. Bone Miner. Res.* **27,** 575–585
52. Chen, L., Xu, Y., Zhao, J., Zhang, Z., Yang, R., Xie, J., Liu, X., and Qi, S. (2014) Conditioned medium from hypoxic bone marrow-derived mesenchymal stem cells enhances wound healing in mice. *PLoS One* **9,** e96161
53. Bussche, L., and Van de Walle, G. R. (2014) Peripheral blood-derived mesenchymal stromal cells promote angiogenesis via paracrine stimulation of vascular endothelial growth factor secretion in the equine model. *Stem Cells Transl. Med.* **3,** 1514–1525
54. Crampton, S. P., Wu, B., Park, E. J., Kim, J.-H., Solomon, C., Waterman, M. L., and Hughes, C. C. (2009) Integration of the β-catenin-dependent Wnt pathway with integrin signaling through the adaptor molecule Grb2. *PLoS One* **4,** e7841
55. Lang, M., Borgmann, M., Oberhuber, G., Evstatiev, R., Jimenez, K., Dammann, K. W., Jambrich, M., Khare, V., Campregher, C., Ristl, R., and Gasche, C. (2013) Thymoquinone attenuates tumor growth in ApcMin mice by interference with Wnt-signaling. *Mol. Cancer* **12,** 41
56. Valapala, M., and Vishwanatha, J. K. (2011) Lipid raft endocytosis and exosomal transport facilitate extracellular trafficking of annexin A2. *J. Biol. Chem.* **286,** 30911–30925
57. González-Sancho, J. M., Brennan, K. R., Castelo-Soccio, L. A., Brown, A. M. (2004) Wnt proteins induce dishevelled phosphorylation via an LRP5/6- independent mechanism, irrespective of their ability to stabilize beta-catenin. *Mol. Cell Biol.* **24,** 4757–4768